INTERNATIONAL JOURNAL FOR NUMERICAL METHODS IN ENGINEERING, VOL. 29, 1135–1158 (1990)

HYPERSINGULAR INTEGRALS IN BOUNDARY ELEMENT FRACTURE ANALYSIS

L. J. GRAY*

IBM Bergen Scientific Centre, Thormøhlensgate 55, 5008 Bergen, Norway

LUIZ F. MARTHA AND A. R. INGRAFFEA

Department of Structural Engineering and Program of Computer Graphics, Cornell University, Ithaca, New York 14853, U.S.A.

SUMMARY

A new general purpose boundary element method for domains with cracks has been recently developed. This technique avoids the use of a multi-domain decomposition by including an additional integral equation expressing the boundary condition on the crack. The principal requirement of this technique is the analytic determination of certain hypersingular integrals of the Green's function which arise from this equation. In order to establish the applicability of this method for fracture, these integrals are evaluated herein for the Kelvin solution of the three-dimensional Navier equations of linear elasticity. Numerical results for fracture problems using the single-domain boundary element analysis are also presented.

INTRODUCTION

A significant problem in the numerical simulation of crack growth[1] has been the need to rediscretize the region as the crack propagates. This requires either a time consuming manual intervention or the development of an intelligent scheme for automatic remeshing. In view of the special care and treatment required at the crack edge,[2] this is an especially difficult task. Although obviously worse within finite elements, wherein the entire volume around the crack must be decomposed, this is nevertheless a serious problem for boundary element simulations, especially in three dimensions. A variety of algorithms for crack problems has been employed with more or less success,[3–6] but the only general purpose, direct boundary element technique for treating cracks has been the multi-domain[7,8] approach. This method, illustrated in Figure 1(a), decomposes the domain into regions without cracks at the expense of introducing extra internal nodes and elements connecting the crack to the outer boundary. As the crack propagates, this mesh between the crack front and the other boundary surfaces must be updated.

The analysis of structures containing many cracks is also an exceedingly difficult numerical problem. Studies of flow in fractured rock masses[9] and stress analysis of concrete dams[10] are two specific applications which naturally give rise to complicated multi-crack geometries. For a realistic three-dimensional model, constructing a multi-domain boundary element or a finite element discretization is clearly laborious, and the ensuing calculation is likely to be prohibitively expensive.

*Permanent address: Mathematical Sciences Section, Engineering Physics and Mathematics Division, Oak Ridge National Laboratory, Oak Ridge, TN 37831, U.S.A.

0029–5981/90/061135–24$12.00

Received 28 March 1989
Revised 3 August 1989

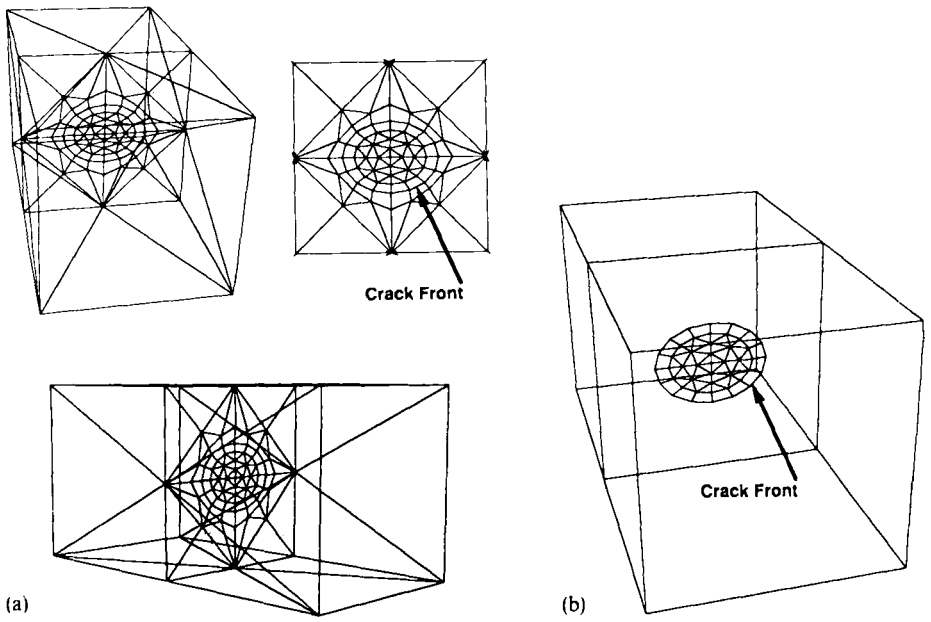

Figure 1. Comparison between multi- and single-domain BEM crack representations: (a) multi-domain mesh; (b) single-domain mesh

Recently, however, a boundary element approach capable of treating cracks without the use of internal surfaces has been developed.[11] Although the basic formalism is completely general, this method has thus far only been applied in potential theory (Laplace's equation), specifically electroplating[12,13] and steady-state heat transfer.[14] The essential ingredient of this method is the analytic evaluation of singular integrals arising from a boundary integral equation expressing the normal derivative (e.g. traction) on the surface. These integrals involve two derivatives of the Green's function (fundamental solution), and are therefore more singular than the usual boundary element integrals: they have been termed *hypersingular*. There has been considerable discussion in the recent literature concerning the treatment of these integrals (see References 15–17 and the papers cited therein), with a 'finite part' evaluation apparently the most widely used method for fracture applications.[16] In this paper, these integrals are treated in a straightforward manner as a limit from the interior of the region. As shown previously for the Laplace equation,[11] this process leads to well defined finite values for the integrals. Although the details are somewhat different, this limiting approach is basically the same as that adopted by Rudolphi *et al.*[15]

Figure 1 shows a comparison between a multi-domain representation for a three-dimensional, elliptical crack and a single-domain representation using the method described in this paper. It is obvious that the size of the problem and the mesh generation effort have substantially decreased. Visualization of both the model and the results is enhanced. Moreover, if simulation of the growth of this crack is sought, the proposed method requires only modification of the crack mesh itself.

This paper will derive the relevant hypersingular integrals of the Green's function for three-dimensional linear elasticity. Not surprisingly, these formulas are very similar to those of the three-dimensional Laplace equation:[11] the fundamental (Kelvin) solution for the displacement is the r^{-1} point source potential plus an additional term. However, displacement and traction are vector quantities; this, together with the presence of the extra term, makes the derivation

considerably more complicated and time consuming. The expressions for the hypersingular integrals are tabulated here so that other people will be spared this somewhat tedious exercise. A complete discussion of the implementation of these formulas for fracture mechanics problems, together with further test calculations, will appear elsewhere.[18]

Defining the hypersingular integral as a limit is fundamentally different from previous methods for assigning a value to this quantity. By placing the singular point directly on the boundary, past techniques had to contend with the presence of singular terms and dispose of them in some fashion. In contrast, there are no singular terms in using the limit process: interior traction values, computed by *integrating over the entire boundary*, are finite and will have a finite limit as the boundary is approached. Terms which might appear to be singular cancel out in the complete integration, before one proceeds to the boundary. In addition to avoiding singular terms, the limiting procedure also provides a sensible interpretation of displacement derivatives parallel to the boundary surface. As in potential theory (and as shown below), these derivatives will give rise to terms which are discontinuous when crossing the boundary (i.e. the limiting value depends upon which side of the surface one is on), and are therefore undefined on the surface itself. While this is no problem if the hypersingular integral is defined as a limit (one must merely specify either an interior or exterior approach), it must clearly cause problems if the singular integral is attacked directly.

In the calculations, the required integration over the entire boundary (to compute the interior traction) imposes a constraint that the representation of the displacement on the crack surface be differentiable.[15,17] As a consequence, standard boundary element interpolation methods do not suffice. A technique for satisfying this constraint can be found in Reference 17, and its implementation for fracture will be discussed in the forthcoming paper cited above.[18]

LINEAR TERMS

The development of the integral equation approach to elasticity was initiated by Rizzo[19] and Cruse;[20] the notation and boundary element formulation employed herein will follow that of Mukherjee.[21] Assuming no body forces, the boundary element integral equation for elasticity relates surface displacements $u_i(P)$ and tractions $\tau_i(P)$ by

$$c_{ij}(P)u_i(P)=\int_{\partial B}[U_{ij}(P,Q)\tau_i(Q)-T_{ij}(P,Q)u_i(Q)]\,ds_Q \tag{1}$$

As is customary, summation over repeated indices is assumed. The coefficient c_{ij} depends upon the local geometry at P; it suffices to assume a smooth crack surface,[13] and in this case $c_{ij}=\delta_{ij}/2$. The functions $U_{ij}(P,Q)$ and $T_{ij}(P,Q)$ are the displacement and traction at a source point P due to a point load at the field point Q in an infinite elastic solid. From Kelvin's solution, these functions are known to be

$$U_{ij}=\frac{1}{16\pi(1-\nu)Gr}\{(3-4\nu)\delta_{ij}+r_{,i}r_{,j}\} \tag{2}$$

$$T_{ij}=-\frac{1}{8\pi(1-\nu)r^2}\left[\{(1-2\nu)\delta_{ij}+3r_{,i}r_{,j}\}\frac{\partial r}{\partial n}+(1-2\nu)(r_{,i}n_j-r_{,j}n_i)\right] \tag{3}$$

where $r=\|P-Q\|$ and $r_{,i}$ denotes a derivative in the direction of the Cartesian basis vector $\mathbf{e}_i$. The basic idea of the present method[11] is to supplement the boundary integral equation (1) with additional equations enforcing the boundary conditions on the crack surface. For the purposes of this paper, it is sufficient to assume that this constraint is zero traction, $\tau_i(P)=0$. As explained

below, this condition forces the consideration of the most singular terms, and there is therefore no loss of generality; other boundary conditions on the crack are accommodated in a similar fashion. In terms of displacement components u_i, the traction at a boundary point P with normal $\mathbf{N}=N_i\mathbf{e}_i$ is given by

$$\tau_i(P)=\sigma_{ij}N_j=G\left\{(u_{i,j}+u_{j,i})N_j+\frac{2\nu}{1-2\nu}u_{k,k}N_i\right\} \tag{4}$$

where ν is the Poisson ratio and G is the shear modulus. Differentiating equation (1) with respect to P (denoted by a capital letter subscript), the traction on the crack boundary can be expressed as

$$0=\tau_i(P)=GN_j\int_{\partial B}[\{U_{mi,J}+U_{mj,I}\}(P,Q)\tau_m(Q)-\{T_{mi,J}+T_{mj,I}\}(P,Q)u_m(Q)]\,\mathrm{d}s_Q$$
$$+\frac{2\nu}{1-2\nu}GN_i\int_{\partial B}\{U_{mk,K}(P,Q)\tau_m(Q)-T_{mk,K}(P,Q)u_m(Q)\}\,\mathrm{d}s_Q \tag{5}$$

where the derivatives of the traction function are given by

$$T_{ij,L}(P,Q)=\frac{1}{8\pi(1-\nu)r^3}\left[3(r_{,i}\delta_{jl}+r_{,j}\delta_{li}-5r_{,l}r_{,i}r_{,j})\frac{\partial r}{\partial n}+3r_{,i}r_{,j}n_l\right.$$
$$\left.+(1-2\nu)\left\{\delta_{ij}n_l-\delta_{jl}n_i+\delta_{li}n_j+3\left(n_ir_{,j}r_{,l}-n_jr_{,l}r_{,i}-r_{,l}\delta_{ij}\frac{\partial r}{\partial n}\right)\right\}\right] \tag{6}$$

and δ_{ij} is the Kronecker delta. It should be pointed out that, as discussed in the previous section, equation (5) will be employed for an *interior* point P, so that the kernels U_{ij} and T_{ij} in equation (1) are well behaved. The derivative therefore exists and can be moved inside the integral as in equation (5). The principal task is to compute the limit of this equation as P approaches the boundary.

The discretization of equation (5) follows the usual boundary element procedure. The integrations over a particular element E are well defined and can be carried out numerically, except when the point P is on E; as P is a node on the crack, singular integrals occur only in the integration over the crack surface ∂C, Figure 2. Utilizing the boundary condition $\tau_m(Q)=0$ on the crack, the non-vanishing integrals over ∂C are

$$-GN_j\int_{\partial C}\{T_{mi,J}(P,Q)+T_{mj,I}(P,Q)\}u_m(Q)\,\mathrm{d}s_Q-\frac{2\nu}{(1-2\nu)}GN_i\int_{\partial C}T_{mk,K}(P,Q)u_m(Q)\,\mathrm{d}s_Q \tag{7}$$

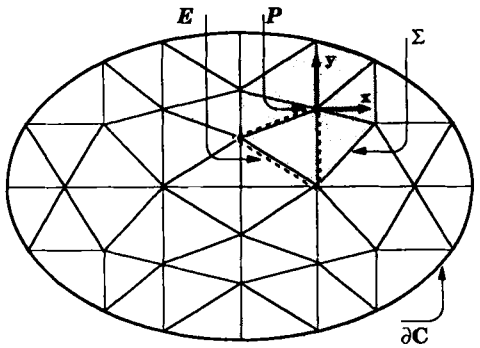

Figure 2. Crack surface, ∂C, and crack node neighbourhood, Σ

Note that the terms which have been dropped from equation (5) because of the zero traction boundary condition involve only one derivative of U. Thus, the singular integrals arising from other boundary conditions are no more singular than standard boundary element integrals, and there is consequently no loss of generality in examining equation (7).

The singular integrals arising from equation (7) will be evaluated analytically using a local co-ordinate system centred at P. As with the Laplace equation,[11] these integrals can be assigned a finite value by integrating over a surface patch Σ having P as an interior point. For convenience, it will be assumed that Σ lies in the x–y plane; thus, $\mathbf{N}=(0, 0, 1)$ and the $\partial r/\partial n$ term in equation (6) is $\partial r/\partial z$ everywhere on Σ. As discussed above, if the singular point P is moved off the surface, $P=(0, 0, z_0)$, the integrals over Σ are well defined, and the limit as $z_0 \to 0$ can then be considered. Polar co-ordinates (ρ, θ) will be used in the x–y plane, and in terms of these co-ordinates the neighbourhood Σ can be described by $0 \leqslant \rho \leqslant \hat{\rho}(\theta)$, $0 \leqslant \theta \leqslant 2\pi$.

The approximation of the displacement in equation (7) is of importance. As mentioned above (and as will be seen from the calculations below), the representation of u_m for the hypersingular integral cannot utilize standard techniques. The difference between this situation and the usual boundary element implementation is illustrated in Figure 3. In this example, the neighbourhood surrounding the crack node P is composed of six triangular elements. In a simple linear element calculation, the displacement field would be approximated by different linear functions on each element. If these functions are chosen to interpolate the nodal values of u_m, then the representation will be continuous on Σ, but not differentiable across the element edges. Correct treatment of the hypersingular integral requires differentiability. The method described in Reference 17 utilizes, as shown in Figure 3(b), a single polynomial over Σ to achieve this goal. This polynomial will contain terms beyond linear, and thus the integration of these terms must also be considered.

There are implicit assumptions in the above description of Σ as, except for a flat crack, this simple geometry will not be valid. Even if planar elements are employed in the discretization of ∂C, the neighbourhood Σ of a crack node P will not in general be planar and the normal $\mathbf{N}$ at the crack node P will not necessarily coincide with the normal to the element E. As a consequence, it is also necessary to consider derivatives parallel to the crack surface; these terms will be dealt with in a subsequent section. A more troublesome consequence of the above treatment is that the formulas to be derived apply only to planar elements. This means that, currently, a curved crack surface must be represented by planar elements. Curved elements present an additional level of complexity in obtaining appropriate formulas for the singular integrals (the surface normal $\mathbf{n}$ is not constant), but do not present any mathematical difficulties in the existence of the limit to the surface. As found below, potential singular terms (which turn out to be of the form $\log(z_0)$) are localized exactly at the singular point (i.e. independent of $\hat{\rho}(\theta)$). Since any smooth surface is locally flat, the limit analysis will therefore hold in this more general setting. Derivation of appropriate formulas for curved elements will be left to the future.

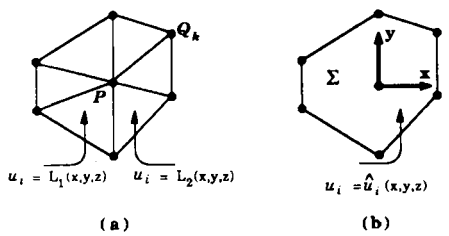

Figure 3. The neighbourhood of a crack node, illustrating the (a) piecewise line and (b) differentiable approximations

1. $i=1, m=1$

The calculation of this first term will be presented in full detail; for this initial choice of subscripts, equation (7) simplifies to

$$-G\int_{\Sigma}\{T_{11,3}(P,Q)+T_{13,1}(P,Q)\}u_1(Q)\,ds_Q \tag{8}$$

from equation (6)

$$\begin{aligned} T_{11,3}&=\frac{1}{8\pi(1-\nu)}\frac{1}{r^3}[-15r_{,1}r_{,1}r_{,3}r_{,3}+3r_{,1}r_{,1}+(1-2\nu)\{1-3r_{,3}r_{,3}\}]\\ T_{13,1}&=\frac{1}{8\pi(1-\nu)}\frac{1}{r^3}[-15r_{,1}r_{,1}r_{,3}r_{,3}+3r_{,3}r_{,3}+(1-2\nu)\{1-3r_{,1}r_{,1}\}] \end{aligned} \tag{9}$$

The displacement $u_m(Q)$ on the surface Σ is, as usual, approximated in terms of nodal values. For the discussion of the potentially singular terms which arise out of equation (7), it suffices to consider the linear terms

$$u_m(\rho,\theta)=a_m+b_m\rho\cos(\theta)+c_m\rho\sin(\theta) \tag{10}$$

where the coefficients $\{a_m, b_m, c_m\}$ are linear combinations of the displacements at the nodes defining Σ. Higher order terms, to be considered in the next section, turn out to be well behaved. With u_1 as above and $\kappa_1=-G(8\pi(1-\nu))^{-1}$, equation (8) can be written

$$\begin{aligned} \kappa_1\int_{\Sigma}\frac{1}{r^3}&[-30r_{,1}r_{,1}r_{,3}r_{,3}+2+2\nu\{2-3r_{,3}r_{,3}-3r_{,1}r_{,1}\}]\\ &\times(a_1+b_1\rho\cos(\theta)+c_1\rho\sin(\theta))\rho\,d\rho d\theta \end{aligned} \tag{11}$$

Noting that $r_{,1}=x/r=\rho\cos(\theta)/r$, $r_{,3}=-z_0/r$ and $r=(\rho^2+z_0^2)^{1/2}$, the coefficient of a_1 in equation (11) is given by

$$\begin{aligned} \kappa_1\int_0^{2\pi}d\theta\int_0^{\hat{\rho}(\theta)}&\left[\frac{-30\rho^2\cos^2(\theta)z_0^2}{r^7}+\frac{3z_0^2}{r^5}+\frac{3\rho^2\cos^2(\theta)}{r^5}\right.\\ &\left.+(1-2\nu)\left\{\frac{2}{r^3}-\frac{3z_0^2}{r^5}-\frac{3\rho^2\cos^2(\theta)}{r^5}\right\}\right]\rho\,d\rho \end{aligned} \tag{12}$$

The integrals over ρ are easily evaluated with the use of integral tables; the relevant integration formulas[22] have been collected in the Appendix. The coefficient of a_1 is then

$$\begin{aligned} \kappa_1\int_0^{2\pi}d\theta&\left[-30\cos^2(\theta)z_0^2\left\{\frac{-1}{3\hat{R}^3}+\frac{z_0^2}{5\hat{R}^5}+\frac{2}{15z_0^3}\right\}\right.\\ &+3z_0^2\left\{\frac{-1}{3\hat{R}^3}+\frac{1}{3z_0^3}\right\}+3\cos^2(\theta)\left\{\frac{-1}{\hat{R}}+\frac{z_0^2}{3\hat{R}^3}+\frac{2}{3z_0}\right\}\\ &+(1-2\nu)\left\{\frac{-2}{\hat{R}}+\frac{2}{z_0}-3z_0^2\left(\frac{-1}{3\hat{R}^3}+\frac{1}{3z_0^3}\right)\right.\\ &\left.\left.-3\cos^2(\theta)\left(\frac{-1}{\hat{R}}+\frac{z_0^2}{3\hat{R}^3}+\frac{2}{3z_0}\right)\right\}\right] \end{aligned} \tag{13}$$

where $\hat{R}=(\hat{\rho}(\theta)^2+z_0^2)^{1/2}$ The terms which are singular in the limit $z_0\to 0$ are of the form z_0^{-1} and sum to

$$\frac{1}{4\pi z_0}\int_0^{2\pi} d\theta\{2\cos^2(\theta)-1\}=0 \tag{14}$$

so, as desired, the singularity drops out after integration over θ. This is the expected behaviour and will indeed occur in all subsequent calculations. Thus, as discussed in the introduction, there are no singular terms present in the interior traction contributions which might cause problems in approaching the boundary. Many of the remaining terms in equation (13) have a positive power of z_0 and thus also disappear in the limit $z_0\to 0$; as $\hat{R}\to\hat{\rho}(\theta)$ the coefficient of a_1 becomes

$$-\kappa_1\int_0^{2\pi}\left\{\frac{2(1-2\nu)+6\nu\cos^2(\theta)}{\hat{\rho}(\theta)}\right\}d\theta \tag{15}$$

The integral for the coefficient of b_1 is the same as equation (12) with an additional factor of $\rho\cos(\theta)$, yielding

$$\kappa_1\int_0^{2\pi} d\theta\cos(\theta)\int_0^{\hat{\rho}(\theta)}\left[\frac{-30\rho^2\cos^2(\theta)z_0^2}{r^7}+\frac{3z_0^2}{r^5}+\frac{3\rho^2\cos^2(\theta)}{r^5}\right.$$
$$\left.+(1-2\nu)\left\{\frac{2}{r^3}-\frac{3z_0^2}{r^5}-\frac{3\rho^2\cos^2(\theta)}{r^5}\right\}\right]\rho^2\,d\rho \tag{16}$$

Replacing the outside $\cos(\theta)$ factor with $\sin(\theta)$, one obtains the corresponding integral multiplying c_1, so these terms are easily evaluated at the same time. Integrating over ρ yields

$$\kappa_1\int_0^{2\pi} d\theta\cos(\theta)\left[\frac{-6\cos^2(\theta)\rho^5}{\hat{R}^5}+\frac{\rho^3}{\hat{R}^3}-3\cos^2(\theta)\left(\frac{\hat{\rho}(\theta)}{\hat{R}}+\frac{\hat{\rho}(\theta)^3}{3\hat{R}^3}-\log(\hat{\rho}(\theta)+\hat{R})+\log|z_0|\right)\right.$$
$$+(1-2\nu)\left\{2\left(\frac{-\hat{\rho}(\theta)}{\hat{R}}+\log(\hat{\rho}(\theta)+\hat{R})-\log|z_0|\right)\right.$$
$$\left.\left.-\frac{\hat{\rho}^3}{\hat{R}^3}-3\cos^2(\theta)\left(\frac{-\hat{\rho}(\theta)}{\hat{R}}+\frac{-\hat{\rho}(\theta)^3}{3\hat{R}^3}+\log(\hat{\rho}(\theta)+\hat{R})-\log|z_0|\right)\right\}\right] \tag{17}$$

The $\log|z_0|$ term is singular as $z_0\to 0$, but the coefficients $\cos(\theta)$ or $\cos^3(\theta)$ ($\sin(\theta)$ and $\sin(\theta)\cos^2(\theta)$ in the case of c_1) integrate to 0 over θ, so these terms disappear. Note too that $\hat{R}\to\hat{\rho}(\theta)$, and that all terms with powers of $\hat{\rho}(\theta)/\hat{R}$ have coefficients which also integrate to zero. These terms therefore also vanish in the limit, leaving

$$\kappa_1\int_0^{2\pi}\{2(1-2\nu)\cos(\theta)+6\nu\cos^3(\theta)\}\log(2\hat{\rho}(\theta))\,d\theta \tag{18a}$$

$$\kappa_1\int_0^{2\pi}\{2(1-2\nu)\sin(\theta)+6\nu\sin(\theta)\cos^2(\theta)\}\log(2\hat{\rho}(\theta))\,d\theta \tag{18b}$$

for the coefficients of b_1 and c_1, respectively. The integrals appearing in equations (15) and (18) can be evaluated in closed form; for a triangular element (and Laplace's equation); these details have been worked out in Reference 11. This completes the discussion of the linear terms for $i=m=1$; for the remaining cases, the analysis follows along similar lines and fewer details will be provided.

2. $i=1$, $m=2$

Using equations (6), (7) and (10), the coefficient of a_2, analogous to equation (12) for a_1, is expressed as

$$\kappa_1 \int_0^{2\pi} d\theta \left[\int_0^{\hat{\rho}(\theta)} \frac{-30\rho^2 \cos(\theta)\sin(\theta) z_0^2}{r^7} + \frac{6\nu \cos(\theta)\sin(\theta)\rho^2}{r^5} \rho \, d\rho \right] \tag{19}$$

Performing the integrals over ρ, one sees again that the singular z_0^{-1} terms disappear after integration over θ; the only non-vanishing term in the limit is

$$\frac{6\nu}{8\pi(1-\nu)} \int_0^{2\pi} \frac{\cos(\theta)\sin(\theta)}{\hat{\rho}(\theta)} d\theta \tag{20a}$$

As before, the coefficients of b_2 and c_2 are obtained from equation (19) by including a factor of $\rho\cos(\theta)$ or $\rho\sin(\theta)$. The singular terms are of the form $\log|z_0|$ and, as expected, have coefficients which integrate to zero, leaving

$$\frac{-6\nu}{8\pi(1-\nu)} \int_0^{2\pi} \cos^2(\theta)\sin(\theta)\log(2\hat{\rho}(\theta)) d\theta \tag{20b}$$

$$\frac{-6\nu}{8\pi(1-\nu)} \int_0^{2\pi} \cos(\theta)\sin^2(\theta)\log(2\hat{\rho}(\theta)) d\theta \tag{20c}$$

3. $i=1$, $m=3$

The contribution to the traction in the $\mathbf{e}_1$ direction due to displacement normal to the crack surface (i.e. in the $\mathbf{e}_3$ direction), is known to be zero. This is precisely the result obtained directly from the integrations. The coefficient of a_3 is given by

$$\kappa_1 \int_0^{2\pi} d\theta \left[\int_0^{\hat{\rho}(\theta)} \frac{-30\rho \cos(\theta) z_0^3}{r^7} + \frac{6\cos(\theta)\rho z_0}{r^5} \rho \, d\rho \right] \tag{21}$$

After integrating, it is immediately obvious that all terms vanish in the limit, with the exception of the singular contribution

$$\frac{\kappa_1}{z_0} \int_0^{2\pi} d\theta \left[6\cos(\theta) \frac{\hat{\rho}(\theta)^5}{\hat{R}^5} - 8\cos(\theta) \frac{\hat{\rho}(\theta)^3}{\hat{R}^3} \right] \tag{22}$$

Although this term appears to be singular, note that the integral itself vanishes in the limit: $\hat{\rho}(\theta)/\hat{R} \to 1$ as $z_0 \to 0$ and $\cos(\theta)$ integrates to zero. The limiting behaviour of this term therefore hinges on how fast the integral disappears, and this is easily determined. Using the standard Taylor series,

$$\left[\frac{\hat{\rho}(\theta)}{\hat{R}} \right]^L = \left(1 + \frac{z_0^2}{\hat{\rho}(\theta)^2} \right)^{-L/2} \approx 1 - \frac{L}{2} \frac{z_0^2}{\hat{\rho}(\theta)^2} + \cdots \tag{23}$$

and thus the integral behaves as z_0^2, eliminating the singular z_0^{-1} factor in equation (22). For the coefficients b_3 and c_3 there are no singular terms, and the integral vanishes in the limit. This completes the case $i=1$.

4. $i=2$, $1 \leqslant m \leqslant 3$

Not surprisingly, the situation for $i=2$ is analogous to $i=1$, and can be dispensed with in short order. For $m=1$ the results are precisely the same as $i=1$, $m=2$ (equation (20)); the case $m=2$ is

the same as $i=m=1$, provided that $r_{,1}$ in equation (11) is replaced by $r_{,2}$. This amounts to replacing $\cos(\theta)$ with $\sin(\theta)$ in equation (12), and thus, mimicking equations (15) and (18), one obtains

$$-\kappa_1 \int_0^{2\pi} \frac{2(1-2\nu)+6\nu\sin^2(\theta)}{\hat{\rho}(\theta)}\,d\theta \tag{24a}$$

$$\kappa_1 \int_0^{2\pi} \{2(1-2\nu)\cos(\theta)+6\nu\cos(\theta)\sin^2(\theta)\}\log(2\hat{\rho}(\theta))\,d\theta \tag{24b}$$

$$\kappa_1 \int_0^{2\pi} \{2(1-2\nu)\sin(\theta)+6\nu\sin(\theta)\sin^2(\theta)\}\log(2\hat{\rho}(\theta))\,d\theta \tag{24c}$$

for the coefficients of a_2, b_2, c_2, respectively. As with $i=1$, $m=3$, the case $i=2$, $m=3$ also yields a result of zero.

5. $i=3$, $m=1$

The integrals for $i=3$ are quite naturally different from those encountered already; the second half of equation (7) now comes into play, and the terms are even lengthier than before. For this first case, equation (7) becomes

$$\kappa_2 \int_0^{2\pi} d\theta \int_0^{\hat{\rho}(\theta)} \left\{\frac{-15\rho\cos(\theta)z_0^3}{r^7}+\frac{(3+6\nu)\rho\cos(\theta)z_0}{r^5}\right\}\rho\,d\rho$$
$$+\nu\kappa_2 \int_0^{2\pi} d\theta \int_0^{\hat{\rho}(\theta)} \left\{\frac{-15\rho(\rho^2-z_0^2)\cos(\theta)z_0}{r^7}+\frac{3\rho\cos(\theta)z_0}{r^5}\right\}\rho\,d\rho \tag{25}$$

where $\kappa_2=-2[8\pi(1-\nu)(1-2\nu)]^{-1}$. After integration the coefficient of a_1 is found to be

$$\frac{\kappa_2}{z_0}\int_0^{2\pi} d\theta\cos(\theta)\left[\frac{(3-6\nu)\hat{\rho}(\theta)^5}{\hat{R}^5}+\frac{(-4+3\nu)\hat{\rho}(\theta)^3}{\hat{R}^3}\right] \tag{26}$$

Using equation (23), it is easily seen that this term vanishes with z_0, as expected. The coefficients of b_1 and c_1 work out slightly differently. Obtaining the integrals from equation (25) in the usual fashion and performing the complete integration, one finds that the first integral in equation (25) has a non-zero value of $4\pi\nu\kappa_2$. The second integral, however, exactly cancels with this result, and the correct result is obtained.

6. $i=3$, $m=2$

As before, exchanging the appropriate $\cos(\theta)$ terms with $\sin(\theta)$ ($r_{,2}$ replacing $r_{,1}$ in equation (25)), the above analysis carries over to this new term, and thus the results remain zero.

7. $i=3$, $m=3$

From the basic equation (7), this contribution can be expressed as

$$-2G\int_\Sigma T_{33,3}u_3(Q)\,ds_Q-\frac{2\nu}{1-2\nu}G\int_\Sigma\{T_{31,1}+T_{32,2}+T_{33,3}\}u_3(Q)\,ds_Q \tag{27}$$

For the coefficient of a_3, the *first* integral above becomes

$$2\kappa_1 \int_0^{2\pi} d\theta \int_0^{\hat{\rho}(\theta)} \left[\frac{(6+6\nu)z_0^2}{r^5} - \frac{15z_0^4}{r^7} + \frac{(1-2\nu)}{r^3} \right] \rho \, d\rho \tag{28}$$

The singular terms from this integral, of the form z_0^{-1}, cancel out, and the non-vanishing terms in the limit reduce to

$$-2\kappa_1 \int_0^{2\pi} \frac{d\theta}{\hat{\rho}(\theta)} \tag{29}$$

The singular terms in the second integral in equation (27) also cancel, but in this case there are no surviving terms. Thus, equation (29) is the total contribution. For the b_3 and c_3 coefficients, the singularity is again logarithmic and once again the integration over θ nicely removes it. As with a_3, the first integral in equation (27) provides the entire contribution, which for b_3 is

$$2\kappa_1 \int_0^{2\pi} \cos(\theta) \log(2\hat{\rho}(\theta)) \, d\theta \tag{30a}$$

and

$$2\kappa_1 \int_0^{2\pi} \sin(\theta) \log(2\hat{\rho}(\theta)) \, d\theta \tag{30b}$$

for c_3. This completes the discussion of the singular integral terms which arise from the present method; the results are summarized in Table I.

HIGHER ORDER TERMS

As indicated by the above computations and as discussed in detail elsewhere,[17] an implicit assumption in the singular integral derivations is that the functional form for the displacement $u_m(Q)$ (equation (10)) is valid on a *neighbourhood* of the singular point P. The calculations must therefore treat this neighbourhood consistently, utilizing the same representation of u_m on every element containing P. As a consequence, even if linear triangular elements are employed everywhere else in the calculation, higher order terms can, and should, be used in conjunction with the crack equation (5). In this section, the contributions arising from quadratic and cubic terms will be obtained. The exponent of ρ in these terms is sufficiently high that there is no remaining trace of the singularity.

The quadratic terms will be dealt with first,

$$u_m(\rho, \theta) = \cdots + d_m \rho^2 \cos^2(\theta) + e_m \rho^2 \cos(\theta) \sin(\theta) + f_m \rho^2 \sin^2(\theta) + \cdots \tag{31}$$

Taking all the terms together, the integrals corresponding to equation (12) for $i = m = 1$ take the form

$$\kappa_1 \int_0^{2\pi} d\theta \begin{Bmatrix} \cos^2(\theta) \\ \cos(\theta)\sin(\theta) \\ \sin^2(\theta) \end{Bmatrix} \int_0^{\hat{\rho}(\theta)} \left[\frac{-30\rho^2 \cos^2(\theta) z_0^2}{r^7} + \frac{3z_0^2}{r^5} + \frac{3\rho^2 \cos^2(\theta)}{r^5} \right.$$
$$\left. + (1-2\nu) \left\{ \frac{2}{r^3} - \frac{3z_0^2}{r^5} - \frac{3\rho^2 \cos^2(\theta)}{r^5} \right\} \right] \rho^3 \, d\rho \tag{32}$$

Table I. Singular integrals: linear terms $u_m(x, y) = a_m + b_m x + c_m y + \cdots$; $\kappa_1 = -G[8\pi(1-\nu)]^{-1}$

	a_1: $-\kappa_1 \int_0^{2\pi} (2(1-2\nu)+6\nu\cos^2(\theta))(\hat{\rho}(\theta))^{-1}\,d\theta$	a_2: $-6\nu\kappa_1 \int_0^{2\pi} \cos(\theta)(\hat{\rho}(\theta))^{-1}\,d\theta$	a_3: 0
$i=1$	b_1: $\kappa_1 \int_0^{2\pi} \cos(\theta)(2(1-2\nu)+6\nu\cos^2(\theta))\log(2\hat{\rho}(\theta))\,d\theta$	b_2: $6\nu\kappa_1 \int_0^{2\pi} \cos^2(\theta)\sin(\theta)\log(2\hat{\rho}(\theta))\,d\theta$	b_3: 0
	c_1: $\kappa_1 \int_0^{2\pi} \sin(\theta)(2(1-2\nu)+6\nu\cos^2(\theta))\log(2\hat{\rho}(\theta))\,d\theta$	c_2: $6\nu\kappa_1 \int_0^{2\pi} \cos(\theta)\sin^2(\theta)\log(2\hat{\rho}(\theta))\,d\theta$	c_3: 0
	a_1: $-6\nu\kappa_1 \int_0^{2\pi} \cos(\theta)\sin(\theta)(\hat{\rho}(\theta))^{-1}\,d\theta$	a_2: $-\kappa_1 \int_0^{2\pi} (2(1-2\nu)+6\nu\sin^2(\theta))(\hat{\rho}(\theta))^{-1}\,d\theta$	a_3: 0
$i=2$	b_1: $6\nu\kappa_1 \int_0^{2\pi} \cos^2(\theta)\sin(\theta)\log(2\hat{\rho}(\theta))\,d\theta$	b_2: $\kappa_1 \int_0^{2\pi} \cos(\theta)(2(1-2\nu)+6\nu\sin^2(\theta))\log(2\hat{\rho}(\theta))\,d\theta$	b_3: 0
	c_1: $6\nu\kappa_1 \int_0^{2\pi} \cos(\theta)\sin^2(\theta)\log(2\hat{\rho}(\theta))\,d\theta$	c_2: $\kappa_1 \int_0^{2\pi} \sin(\theta)(2(1-2\nu)+6\nu\sin^2(\theta))\log(2\hat{\rho}(\theta))\,d\theta$	c_3: 0
	a_1: 0	a_2: 0	a_3: $-2\kappa_1 \int_0^{2\pi} (\hat{\rho}(\theta))^{-1}\,d\theta$
$i=3$	b_1: 0	b_2: 0	b_3: $2\kappa_1 \int_0^{2\pi} \cos(\theta)\log(2\hat{\rho}(\theta))\,d\theta$
	c_1: 0	c_2: 0	c_3: $2\kappa_1 \int_0^{2\pi} \sin(\theta)\log(2\hat{\rho}(\theta))\,d\theta$

where it is understood that the $\cos^2(\theta)$ factor in the θ integral is associated with the d_m term, etc. The trailing factor ρ^3 is now sufficiently strong that all terms with a factor of z_0 will vanish in the limit. After integration the remaining terms yield

$$\kappa_1 \int_0^{2\pi} d\theta \begin{Bmatrix} \cos^2(\theta) \\ \cos(\theta)\sin(\theta) \\ \sin^2(\theta) \end{Bmatrix} \left[3\cos^2(\theta)\left\{\hat{R} + \frac{2z_0^2}{\hat{R}} - \frac{z_0^4}{3\hat{R}^3} - \frac{8z_0}{3}\right\} + (1-2\nu)\left\{2\left(\hat{R} + \frac{z_0^2}{\hat{R}} - 2z_0\right) - 3\cos^2(\theta)\left(\hat{R} + \frac{2z_0^2}{\hat{R}} - \frac{z_0^4}{3\hat{R}^3} - \frac{8z_0}{3}\right)\right\}\right] \tag{33}$$

In the limit, the coefficients reduce to

$$\kappa_1 \int_0^{2\pi} \begin{Bmatrix} \cos^2(\theta) \\ \cos(\theta)\sin(\theta) \\ \sin^2(\theta) \end{Bmatrix} \{2(1-2\nu) + 6\nu\cos^2(\theta)\}\hat{\rho}(\theta)\,d\theta \tag{34}$$

As in the discussion of the linear terms in the previous section, most of the details of the calculations for the subsequent terms will be omitted. For $i=1, m=2$, there is only one term in the integrand without a z_0 factor, and integrating over ρ this term becomes

$$6\nu\kappa_1 \int_0^{2\pi} \begin{Bmatrix} \cos^2(\theta) \\ \cos(\theta)\sin(\theta) \\ \sin^2(\theta) \end{Bmatrix} \cos(\theta)\sin(\theta)\hat{\rho}(\theta)\,d\theta \tag{35}$$

For $m=3$, the result, as expected, is zero.

The case $i=2$ is quickly disposed of: $m=1$ yields equation (35) once again, $m=2$ is easily obtained from equation (34),

$$\kappa_1 \int_0^{2\pi} \begin{Bmatrix} \cos^2(\theta) \\ \cos(\theta)\sin(\theta) \\ \sin^2(\theta) \end{Bmatrix} \{2(1-2\nu) + 6\nu\sin^2(\theta)\}\hat{\rho}(\theta)\,d\theta \tag{36}$$

and $m=3$ yields zero. For $i=3$, $m=1, 2$, all terms have a factor of z_0 and therefore vanish in the limit. The final term, $m=3$, has one non-zero contribution (see equation (28)) given by

$$\kappa_2 \int_0^{2\pi} d\theta \begin{Bmatrix} \cos^2(\theta) \\ \cos(\theta)\sin(\theta) \\ \sin^2(\theta) \end{Bmatrix} \int_0^{\hat{\rho}(\theta)} \frac{(1-2\nu)}{r^3}\rho^3\,d\rho = 2\kappa_1 \int_0^{2\pi} \begin{Bmatrix} \cos^2(\theta) \\ \cos(\theta)\sin(\theta) \\ \sin^2(\theta) \end{Bmatrix} \hat{\rho}(\theta)\,d\theta \tag{37}$$

The integrations for cubic terms

$$u_m(\rho,\theta) = \cdots + \rho^3\{g_m\cos^3(\theta) + h_m\cos^2(\theta)\sin(\theta) + p_m\cos(\theta)\sin^2(\theta) + q_m\sin^3(\theta)\} + \cdots \tag{38}$$

follow in precisely the same fashion: as might be expected, the factor of $\hat{\rho}(\theta)$ appearing in the quadratic integrals is replaced by $\frac{1}{2}\hat{\rho}^2(\theta)$. These results are summarized in Tables II and III.

Table II. Singular integrals: quadratic terms $u_m(x, y) = \cdots + d_m x^2 + e_m xy + f_m y^2 + \cdots$; $\kappa_1 = -G[8\pi(1-\nu)]^{-1}$

	$m=1$	$m=2$	$m=3$
$i=1$	$\kappa_1 \int_0^{2\pi} \begin{Bmatrix} \cos^2(\theta) \\ \cos(\theta)\sin(\theta) \\ \sin^2(\theta) \end{Bmatrix} (2(1-2\nu)+6\nu\cos^2(\theta))\hat{\rho}(\theta)\,d\theta$	$6\nu\kappa_1 \int_0^{2\pi} \begin{Bmatrix} \cos^2(\theta) \\ \cos(\theta)\sin(\theta) \\ \sin^2(\theta) \end{Bmatrix} \cos(\theta)\sin(\theta)\hat{\rho}(\theta)\,d\theta$	0
$i=2$	$6\nu\kappa_1 \int_0^{2\pi} \begin{Bmatrix} \cos^2(\theta) \\ \cos(\theta)\sin(\theta) \\ \sin^2(\theta) \end{Bmatrix} \cos(\theta)\sin(\theta)\hat{\rho}(\theta)\,d\theta$	$\kappa_1 \int_0^{2\pi} \begin{Bmatrix} \cos^2(\theta) \\ \cos(\theta)\sin(\theta) \\ \sin^2(\theta) \end{Bmatrix} (2(1-2\nu)+6\nu\sin^2(\theta))\hat{\rho}(\theta)\,d\theta$	0
$i=3$	0	0	$2\kappa_1 \int_0^{2\pi} \begin{Bmatrix} \cos^2(\theta) \\ \cos(\theta)\sin(\theta) \\ \sin^2(\theta) \end{Bmatrix} \hat{\rho}(\theta)\,d\theta$

Table III. Singular integrals: cubic terms $u_m(x, y) = \cdots + g_m x^3 + h_m x^2 y + p_m x y^2 + g_m y^3 + \cdots$; $\kappa_1 = -G[8\pi(1-\nu)]^{-1}$

	$m=1$	$m=2$	$m=3$
$i=1$	$\kappa_1 \int_0^{2\pi} \begin{Bmatrix} \cos^3(\theta) \\ \cos^2(\theta)\sin(\theta) \\ \cos(\theta)\sin^2(\theta) \\ \sin^3(\theta) \end{Bmatrix} (2(1-2\nu)$ $+6\nu\cos^2(\theta))\tfrac{1}{2}\hat{\rho}^2(\theta)\,d\theta$	$6\nu\kappa_1 \int_0^{2\pi} \begin{Bmatrix} \cos^3(\theta) \\ \cos^2(\theta)\sin(\theta) \\ \cos(\theta)\sin^2(\theta) \\ \sin^3(\theta) \end{Bmatrix} \times \cos(\theta)\sin(\theta)\tfrac{1}{2}\hat{\rho}(\theta)\,d\theta$	0
$i=2$	$6\nu\kappa_1 \int_0^{2\pi} \begin{Bmatrix} \cos^3(\theta) \\ \cos^2(\theta)\sin(\theta) \\ \cos(\theta)\sin^2(\theta) \\ \sin^3(\theta) \end{Bmatrix} \cos(\theta)\sin(\theta)\tfrac{1}{2}\hat{\rho}^2(\theta)\,d\theta$	$\kappa_1 \int_0^{2\pi} \begin{Bmatrix} \cos^3(\theta) \\ \cos^2(\theta)\sin(\theta) \\ \cos(\theta)\sin^2(\theta) \\ \sin^3(\theta) \end{Bmatrix} (2(1-2\nu)$ $+6\nu\sin^2(\theta))\tfrac{1}{2}\hat{\rho}^2(\theta)\,d\theta$	0
$i=3$	0	0	$2\kappa_1 \int_0^{2\pi} \begin{Bmatrix} \cos^3(\theta) \\ \cos^2(\theta)\sin(\theta) \\ \cos(\theta)\sin^2(\theta) \\ \sin^3(\theta) \end{Bmatrix} \tfrac{1}{2}\hat{\rho}^2(\theta)\,d\theta$

TANGENTIAL DERIVATIVES

As mentioned in the discussion of the linear terms, the normal to the crack N at the point P will not in general coincide with the crack element normal. Thus, N_1 and N_2 in equation (7) are not necessarily zero, and all of the integrals derived in the previous two sections must be multiplied by the component N_3. The expressions for tangential derivatives, i.e. those involving N_1 and N_2, behave somewhat differently than does the derivative normal to the crack element. As occurs in potential theory, the tangential derivatives of the surface tractions τ_1 and τ_2 arising from the surface displacements u_1 and u_2 will be found to jump discontinuously at the crack surface, and only the linear coefficients $\{b_1, c_1, b_2, c_2\}$ will contribute. However, the tangential traction contributions from displacement normal to the surface, u_3, are continuous through the crack, and all terms must be examined.

As was done above, the $\tau_1 = 0$ equation will be used to exhibit the basic procedure; subsequent details of the computations will only be provided if deviations from the established pattern arise. From equation (7), the required terms involving u_1 are found to be

$$-GN_1 \int_{\partial C} \left[2T_{11,1} + \frac{2\nu}{(1-2\nu)} \{T_{11,1} + T_{12,2} + T_{13,3}\} \right] u_1$$
$$-GN_2 \int_{\partial C} [T_{11,2} + T_{12,1}] u_1 \, dS \tag{39}$$

and using equation (6), the coefficient of N_1 is given by

$$\kappa_1 \int_{\partial C} \frac{1}{r^3} \left[6(1+2\nu) r_{,1} r_{,3} - 30 r_{,1}^3 r_{,3} + \frac{2\nu}{(1-2\nu)} \{3(3+4\nu) r_{,1} r_{,3} \right.$$
$$\left. - 15 r_{,1} r_{,3} (r_{,1}^2 + r_{,2}^2 + r_{,3}^2)\} \right] u_1 \rho \, d\rho d\theta \tag{40}$$

Performing the required integrations, it is seen that the coefficient of a_1 is composed of terms of the form

$$\frac{1}{z_0} \int_0^{2\pi} f(\theta) \left[\frac{\hat{\rho}(\theta)}{\hat{R}(\theta)} \right]^L d\theta \tag{41}$$

where $\int_0^{2\pi} f(\theta) \, d\theta = 0$ and L is a positive integer. It follows from equation (23) that these terms vanish in the limit $z_0 \to 0$, and the coefficient is therefore zero. The coefficient of b_1 leads to the integral

$$\kappa_1 \int_0^{2\pi} d\theta \cos^2(\theta) \int_0^{\hat{\rho}(\theta)} z_0 \left[-6(1+2\nu) \frac{\rho^3}{r^5} + 15 \cos^2(\theta) \frac{\rho^5}{r^7} \right.$$
$$\left. + \frac{2\nu}{(1-2\nu)} \left\{ -3(3+4\nu) \frac{\rho^3}{r^5} + 15 \left(\frac{\rho^5}{r^7} + z_0^2 \frac{\rho^3}{r^7} \right) \right\} \right] d\rho \tag{42}$$

The important difference from previously encountered terms is that the integrals over ρ, typified by the first term in equation (42),

$$z_0 \int_0^{\hat{\rho}(\theta)} \frac{\rho^3}{r^5} \, d\rho = z_0 \left[\frac{-1}{\hat{R}(\theta)} + \frac{1}{|z_0|} + \frac{z_0^2}{3\hat{R}(\theta)^3} - \frac{z_0^2}{3|z_0|^3} \right] \to \frac{2}{3} \frac{z_0}{|z_0|} \tag{43}$$

are functions of $\psi(z_0) = z_0/|z_0| = \pm 1$ (to an odd power); these are in fact the only surviving

contributions in the limit, and equation (42) reduces to

$$\kappa_1\psi(z_0)\int_0^{2\pi}\cos^2(\theta)\left[-4-8\nu+16\cos^2(\theta)+\frac{2\nu}{(1-2\nu)}(4-8\nu)\right]d\theta=8\pi\kappa_1\psi(z_0) \tag{44}$$

This term therefore depends upon how (i.e. from which side) the point $P=(0, 0, z_0)$ approaches the crack, jumping discontinuously as the crack surface is crossed. As it has been assumed herein that the limit is taken for points P which are interior to the region, $\psi(z_0)=1$ if the positive orientation of the boundary yields an interior normal, and $\psi(z_0)=-1$ for an exterior normal.

The coefficient of c_1 is the same as in equation (44) with the $\cos(\theta)$ factor replaced by $\sin(\theta)$; this term therefore integrates to zero. All higher order terms in u_1 produce, at worst, a logarithmic singularity from the ρ integration, and are consequently disposed of by the z_0 factor. The integral multiplying N_2 in equation (39) is handled in a similar fashion, and all contributions are zero except for the coefficient of c_1 which turns out to be

$$\kappa_1\psi(z_0)\int_0^{2\pi}d\theta\sin(\theta)[4(4-\nu)\sin(\theta)-16\sin^3(\theta)]\,d\theta=4\pi\kappa_1\psi(z_0)(1-\nu) \tag{45}$$

Although the coefficient of u_2 is, with minor variations (see Table IV), the same as above, the coefficient of u_3 is continuous across the crack surface and therefore closely resembles the calculations for the linear terms. This term, defined as

$$-GN_1\int_{\partial C}\left[2T_{31,1}+\frac{2\nu}{(1-2\nu)}\{T_{31,1}+T_{32,2}+T_{33,3}\}\right]u_3$$

$$-GN_2\int_{\partial C}[T_{31,2}+T_{32,1}]u_3\,dS \tag{46}$$

yields the following integral for the coefficient of N_1:

$$\kappa_1\int_0^{2\pi}d\theta\int_0^{\hat\rho(\theta)}\left[6z_0^2\frac{1}{r^5}-30z_0^2\cos^2(\theta)\frac{\rho^2}{r^7}-\frac{2(1-2\nu)}{r^3}+6(1-2\nu)\cos^2(\theta)\frac{\rho^2}{r^5}\right.$$
$$+\frac{2\nu}{(1-2\nu)}\left\{6(2+\nu)z_0^2\frac{1}{r^5}-15z_0^2\left(\frac{\rho^2}{r^7}+z_0^2\frac{1}{r^7}\right)\right.$$
$$\left.\left.-\frac{1-2\nu}{r^3}+3(1-2\nu)\frac{\rho^2}{r^5}\right\}\right]u_3\rho\,d\rho \tag{47}$$

For the coefficient of a_3, all terms from the ρ integration containing a z_0^{-1} singularity vanish in the integration over θ. In a similar fashion for the linear terms, the $\log(|z_0|)$ singularity disappears, leaving

$$-\kappa_1\int_0^{2\pi}[-2+8\nu+6(1-2\nu)\cos^2(\theta)]\frac{1}{\hat\rho(\theta)}\,d\theta \tag{48a}$$

$$\kappa_1\int_0^{2\pi}\cos(\theta)[-2+8\nu+6(1-2\nu)\cos^2(\theta)]\log(2\hat\rho(\theta))\,d\theta \tag{48b}$$

as the coefficients of a_3 and b_3. The calculations for the second (N_2) part of equation (46) follow the same pattern and result in the expressions

$$6(1-2\nu)\kappa_1\int_0^{2\pi}[\cos(\theta)\sin(\theta)]\frac{1}{\hat\rho(\theta)}\,d\theta \tag{49a}$$

Table IV. Tangential derivatives: $\psi(z_0)=z_0/|z_0|=\pm 1$;
$p_C(\theta)=N_1[6\nu\cos^2(\theta)+2(1-2\nu)]+6N_2\nu\cos(\theta)\sin(\theta)$; $p_S(\theta)=N_2[6\nu\sin^2(\theta)+2(1-2\nu)]+6N_1\nu\cos(\theta)\sin(\theta)$;
$q_C(\theta)=N_1[-2+8\nu+6(1-2\nu)\cos^2(\theta)]+6N_2(1-2\nu)\cos(\theta)\sin(\theta)$; $q_S(\theta)=N_2[-2+8\nu+6(1-2\nu)\sin^2(\theta)]+6N_1(1-2\nu)\cos(\theta)\sin(\theta)$

			a_3: $-\kappa_1\int_0^{2\pi} q_C(\theta)(\hat{\rho}(\theta))^{-1}\,d\theta$
$i=1$	b_1: $8\pi N_1\psi(z_0)\kappa_1$	b_2: $4\pi N_2\psi(z_0)\kappa_1(1-\nu)$	$\begin{matrix} b_3 \\ c_3 \end{matrix}$: $\kappa_1\int_0^{2\pi}\begin{Bmatrix}\cos(\theta)\\ \sin(\theta)\end{Bmatrix} q_C(\theta)\log(2\hat{\rho}(\theta))\,d\theta$
	c_1: $4\pi N_2\psi(z_0)\kappa_1(1-\nu)$	c_2: $8\pi N_1\psi(z_0)\kappa_1\nu$	$\begin{matrix} d_3 \\ \vdots \end{matrix}$: $\kappa_1\int_0^{2\pi}\begin{Bmatrix}\cos^2(\theta)\\ \vdots\end{Bmatrix} q_C(\theta)\begin{Bmatrix}\hat{\rho}(\theta)\\ \frac{1}{2}\hat{\rho}^2(\theta)\\ \vdots\end{Bmatrix} d\theta$
			a_3: $-\kappa_1\int_0^{2\pi} q_S(\theta)(\hat{\rho}(\theta))^{-1}\,d\theta$
$i=2$	b_1: $8\pi N_2\psi(z_0)\kappa_1\nu$	b_2: $4\pi N_1\psi(z_0)\kappa_1(1-\nu)$	$\begin{matrix} b_3 \\ c_3 \end{matrix}$: $\kappa_1\int_0^{2\pi}\begin{Bmatrix}\cos(\theta)\\ \sin(\theta)\end{Bmatrix} q_S(\theta)\log(2\hat{\rho}(\theta))\,d\theta$
	c_1: $4\pi N_1\psi(z_0)\kappa_1(1-\nu)$	c_2: $8\pi N_2\psi(z_0)\kappa_1$	$\begin{matrix} d_3 \\ \vdots \end{matrix}$: $\kappa_1\int_0^{2\pi}\begin{Bmatrix}\cos^2(\theta)\\ \vdots\end{Bmatrix} q_S(\theta)\begin{Bmatrix}\hat{\rho}(\theta)\\ \frac{1}{2}\hat{\rho}^2(\theta)\\ \vdots\end{Bmatrix} d\theta$
	a_1: $-\kappa_1\int_0^{2\pi} p_C(\theta)(\hat{\rho}(\theta))^{-1}\,d\theta$	a_2: $-\kappa_1\int_0^{2\pi} p_S(\theta)(\hat{\rho}(\theta)^{-1}\,d\theta$	
$i=3$	$\begin{matrix} b_1 \\ c_1 \end{matrix}$: $\kappa_1\int_0^{2\pi}\begin{Bmatrix}\cos(\theta)\\ \sin(\theta)\end{Bmatrix} p_C(\theta)\log(2\hat{\rho}(\theta))\,d\theta$	$\begin{matrix} b_2 \\ c_2 \end{matrix}$: $\kappa_1\int_0^{2\pi}\begin{Bmatrix}\cos(\theta)\\ \sin(\theta)\end{Bmatrix} p_S(\theta)\log(2\hat{\rho}(\theta))\,d\theta$	0
	$\begin{matrix} d_1 \\ \vdots \end{matrix}$: $\kappa_1\int_0^{2\pi}\begin{Bmatrix}\cos^2(\theta)\\ \vdots\end{Bmatrix} p_C(\theta)\begin{Bmatrix}\hat{\rho}(\theta)\\ \frac{1}{2}\hat{\rho}^2(\theta)\\ \vdots\end{Bmatrix} d\theta$	$\begin{matrix} d_2 \\ \vdots \end{matrix}$: $\kappa_1\int_0^{2\pi}\begin{Bmatrix}\cos^2(\theta)\\ \vdots\end{Bmatrix} p_S(\theta)\begin{Bmatrix}\hat{\rho}(\theta)\\ \frac{1}{2}\hat{\rho}^2(\theta)\\ \vdots\end{Bmatrix} d\theta$	

$$6(1-2\nu)\kappa_1 \int_0^{2\pi} \cos(\theta)[\cos(\theta)\sin(\theta)]\log(2\hat{\rho}(\theta))\,d\theta \tag{49b}$$

As was the case in the previous section, interchanging $\cos(\theta)$ and $\sin(\theta)$ will produce the c_3 coefficient, and the quadratic and cubic terms are obtained from equations (48) and (49) by replacing $\log(\hat{\rho}(\theta))$ with $\hat{\rho}(\theta)$ and $\hat{\rho}(\theta)^2/2$ respectively.

This completes the discussion for $\tau_1 = 0$. As might be expected, the calculations for $\tau_2 = 0$ are exactly analogous to those above, and need not be repeated. The tangential components arising from $\tau_3 = 0$ are given by

$$\begin{aligned} -GN_1 \int_{\partial C} [\{T_{13,1}+T_{11,3}\}u_1 + \{T_{23,1}+T_{21,3}\}u_2 + \{T_{33,1}+T_{31,3}\}u_3]\,dS \\ -GN_2 \int_{\partial C} [\{T_{13,2}+T_{12,3}\}u_1 + \{T_{23,2}+T_{22,3}\}u_2 \\ +\{T_{33,2}+T_{32,3}\}u_3]\,dS \end{aligned} \tag{50}$$

No new situation is encountered in the evaluation of these integrals. The contributions arising from displacements u_1 and u_2 are continuous across the crack and higher order terms are non-zero; the normal displacement u_3 produces no contribution to τ_3. The coefficients of a_1 and a_2 are found to be

$$N_1\kappa_1 \int_0^{2\pi} [2(1-2\nu)+6\nu\cos^2(\theta)]\frac{1}{\hat{\rho}(\theta)}\,d\theta + N_2\kappa_1 \int_0^{2\pi} [6\nu\cos(\theta)\sin(\theta)]\frac{1}{\hat{\rho}(\theta)}\,d\theta \tag{51a}$$

$$N_1\kappa_1 \int_0^{2\pi} [6\nu\cos(\theta)\sin(\theta)]\frac{1}{\hat{\rho}(\theta)}\,d\theta + N_2\kappa_1 \int_0^{2\pi} [2(1-2\nu)+6\nu\sin^2(\theta)]\frac{1}{\hat{\rho}(\theta)}\,d\theta \tag{51b}$$

respectively. The coefficients of the higher order terms can be derived from these expressions by the usual procedure of adding appropriate $\cos(\theta)$ or $\sin(\theta)$ coefficients and replacing $\hat{\rho}(\theta)^{-1}$ by $\log(\hat{\rho}(\theta))$, etc. The results obtained in this section are tabulated in Table IV; note that the zero terms have been omitted from the table.

NUMERICAL RESULTS

The primary focus of this paper has been to formulate the treatment of the hypersingular integral and to develop the formulas in Tables I–IV. To convince the reader that this effort has been worthwhile, results for two simple fracture calculations will be presented. A complete description of the implementation of these formulas is too extensive to be included here,[18] so only the model and results will be discussed.

The test problem, illustrated in Figure 4, is an internal, planar elliptical crack in a constant stress field. Two orientations of the crack will be considered: the first having the crack plane perpendicular to the stress direction ($\gamma = 0$), and the second a configuration in which the plane is rotated about the minor axis of the ellipse 45 degrees ($\gamma = \pi/4$). The stress field is $\sigma = 1$ (stress units), the modulus of elasticity of the material is $E = 10\,000$ (stress units) and the Poisson ratio is $\nu = 0{\cdot}25$. The dimensions of the ellipse are $a = 0{\cdot}25$, $b = 0{\cdot}125$ (units of distance). The mesh adopted on the

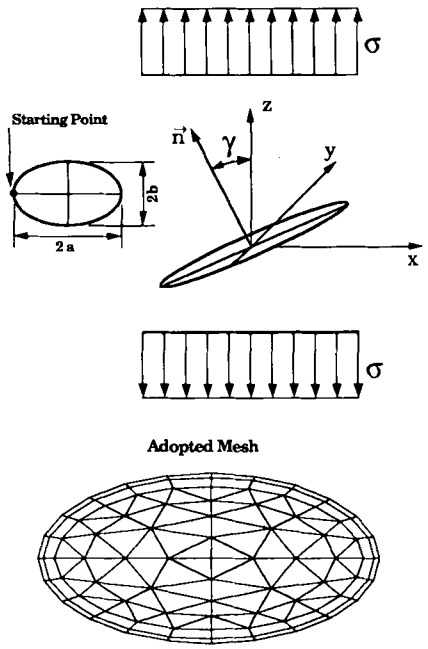

Figure 4. Definitions for benchmark tests of an internal elliptical crack

crack surface is also shown in Figure 4. Surface elements with linear shape functions are employed; the specialized approximation on the crack required for the hypersingular integral employed a cubic polynomial.

A simplified version of the displacement correlation technique[2] has been used to compute the stress intensity factors along the crack front. It is simplified in that it does not use the functional evaluation technique associated with quarter-point elements that was first suggested by Shih *et al.* for the two-dimensional case.[23] These computed values are compared to analytic solutions,[24] and to results obtained from multi-domain analyses with both linear and quadratic elements. The linear multi-domain analysis employed the same mesh shown in Figure 4. The quadratic calculation utilized quarter-point, traction-singular elements along the crack front, and a similar mesh (with the same number of elements along the crack front) was adopted for this calculation. In the computation of stress intensity factors for quadratic elements the same simplification was adopted, and the values were computed based only on displacements at element corner nodes.

A comparison of the results is shown in Figures 5–8. For the orientation $\gamma = 0$, only the Mode I stress intensity factor is non-zero, and these results are plotted in Figure 5. For $\gamma = \pi/4$, Figures 6–8 display Modes I, II and III, respectively. Despite the inherent approximations of the displacement correlation method, the accuracy of the new crack method is evident. In general, these results are nearly as accurate as those from the multi-domain solution employing quarter-point, traction-singular elements. This can be explained by the fact that the new technique, unlike multi-domain or finite element methods, does not get involved in approximating the singular stress field ahead of the crack front. These calculations provide evidence that the potential theory results[12–14] carry over successfully to elasticity.

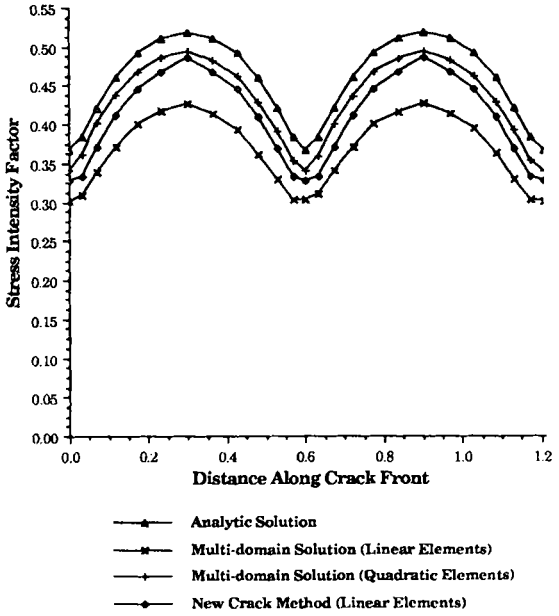

Figure 5. Comparison between the new crack solution, multi-domain method and analytic solution: elliptical crack, Mode I, $\gamma = 0$

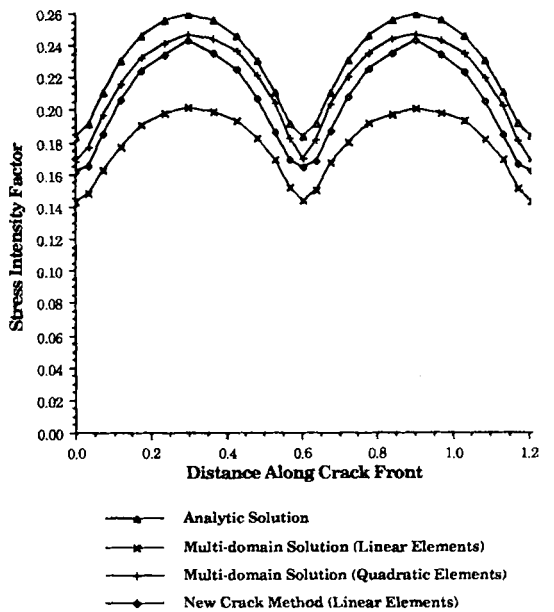

Figure 6. Comparison between the new crack solution, multi-domain method and analytic solution: elliptical crack, Mode I, $\gamma = \pi/4$

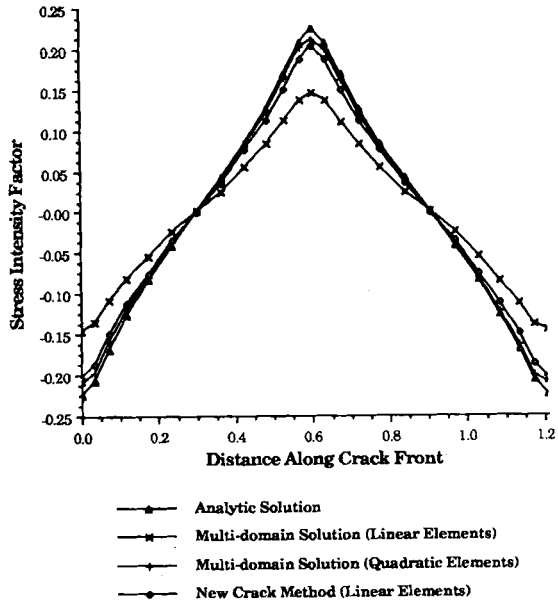

Figure 7. Comparison between the new crack solution, multi-domain method and analytic solution: elliptical crack, Mode II, $\gamma = \pi/4$

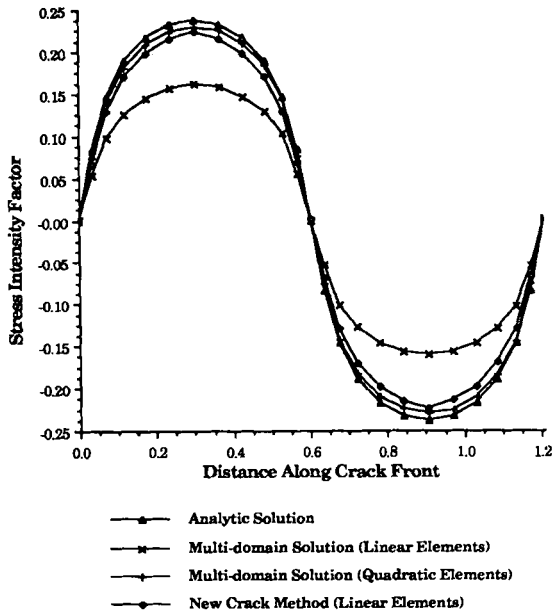

Figure 8. Comparison between the new crack solution, multi-domain method and analytic solution: elliptical crack, Mode III, $\gamma = \pi/4$

CONCLUSIONS

Utilizing the standard Kelvin solution for a point load in an infinite medium, the hypersingular integrals arising from three-dimensional elasticity have been shown to have well defined finite values. Up to now, the general consensus has been that these integrals are intractable for numerical computation.[25,26] The key idea behind this new method is to treat the singular integrals as limits from the interior of the region. As the ability to assign appropriate values to these singular terms is the principal requirement of the present boundary element method,[11,12] there is no impediment in applying this technique to elasticity problems. As indicated by the limited numerical results presented herein, fracture calculations using this technique and (primarily) linear elements (the exception being the special interpolation for the hypersingular integrals) are nearly as accurate as those resulting from a multi-domain calculation using special crack front elements. Since a multi-domain decomposition is not employed, this method will be highly advantageous for crack propagation simulation and difficult multiple crack geometries. More complete details concerning the implementation of this method for the solution of crack problems and more extensive test results can be found elsewhere.[18]

Two observations are worth noting here. First, the proposed method apparently unites the strengths of two alternative boundary element fracture formulations: the direct, Kelvin-solution method and the displacement discontinuity method.[27-29] The former is the most commonly used and, like the present method, readily accommodates finite boundaries. The latter is less widely implemented, but has the advantage of utilizing a straightforward crack representation in the manner exemplified by the discretization shown in Figure 1(b). While there are similarities between the present method and the traction BIE approach,[30] there are some significant differences. By defining the hypersingular integral as a limit and obtaining the analytic expressions in this paper, these troublesome integrals are taken care of in a convenient fashion. As a consequence, the numerical difficulties encountered in the implementation of the traction BIE are not present, and the entire approximation procedure is considerably simpler.

Secondly, with the evaluation of the hypersingular integrals, it should be possible to directly compute the stress everywhere on the boundary surface, in much the same manner that interior values are obtained. This is currently being developed, and a comparison of this approach with a recently proposed method which successfully avoids hypersingular integrals[25] will be carried out.

ACKNOWLEDGEMENTS

This research was sponsored by the IBM Bergen Scientific Centre and the National Science Foundation, NSF Grant No. 8351914. Additional support during the preparation of this article was provided by the Applied Mathematical Sciences Research Program, Office of Energy Research, U.S. Department of Energy under contract DE-AC05-84OR21400 with the Martin Marietta Energy Systems, Inc. The second author acknowledges the support of CNPq, a Brazilian Government agency. Fruitful discussions with Joe Carvalho are appreciated. The implementation of this work was performed at the Program of Computer Graphics, Cornell University.

APPENDIX

For convenience, the integration formulas[22] required in the analysis of the singular integrals are collected here. The notation is the same as above, so that $r=(\rho^2+z_0^2)^{1/2}$.

1. $$\int \frac{\rho}{r^{2p+1}}\,d\rho = -\frac{1}{(2p-1)r^{2p-1}}$$

2. $$\int \frac{\rho^3}{r^{2p+1}}\,d\rho = -\frac{1}{(2p-3)r^{2p-3}} + \frac{z_0^2}{(2p-1)r^{2p-1}}$$

3. $$\int \frac{\rho^5}{r^{2p+1}}\,d\rho = -\frac{1}{(2p-5)r^{2p-5}} + \frac{2z_0^2}{(2p-3)r^{2p-3}} - \frac{z_0^4}{(2p-1)r^{2p-1}}$$

4. $$\int \frac{\rho^4}{r^7}\,d\rho = \frac{1}{5z_0^2}\frac{\rho^5}{r^5}$$

5. $$\int \frac{\rho^2}{r^5}\,d\rho = \frac{1}{3z_0^2}\frac{\rho^3}{r^3}$$

6. $$\int \frac{\rho^4}{r^5}\,d\rho = -\frac{\rho}{r} - \frac{\rho^3}{3r^3} + \log(\rho + r)$$

7. $$\int \frac{\rho^2}{r^3}\,d\rho = -\frac{\rho}{r} + \log(\rho + r)$$

8. $$\int \frac{\rho^2}{r^7}\,d\rho = \frac{1}{z_0^4}\left\{\frac{\rho^3}{3r^3} - \frac{\rho^5}{5r^5}\right\}$$

9. $$\int \frac{\rho^6}{r^5}\,d\rho = \frac{\rho^5}{2r^3} + \frac{10z_0^2\rho^3}{3r^3} + \frac{5z_0^4\rho}{2r^3} - \frac{5}{2}z_0^2\log(\rho + r)$$

10. $$\int \frac{\rho^4}{r^3}\,d\rho = \frac{\rho r}{2} + \frac{z_0^2\rho}{r} - \frac{3}{2}z_0^2\log(\rho + r)$$

11. $$\int \frac{\rho^6}{r^7}\,d\rho = -\frac{23\rho^5}{15r^5} - \frac{7z_0^2\rho^3}{3r^5} - \frac{z_0^4\rho}{r^5} + \log(\rho + r)$$

REFERENCES

1. R. Perucchio and A. R. Ingraffea, 'An integrated boundary element analysis system with interactive computer graphics for three-dimensional linear-elastic fracture mechanics', *Comp. Struct.*, **20**, 157–171 (1985).
2. A. R. Ingraffea and C. Manu, 'Stress-intensity factor computation in three dimensions with quarter-point elements', *Int. j. numer. methods eng.*, **15**, 1427–1445 (1980).
3. T. A. Cruse, 'Boundary-integral equation fracture mechanics analysis', in T. A. Cruse and F. J. Rizzo (eds.), *Boundary-Integral Equation Method: Computational Applications in Applied Mechanics*, ASME Appl. Mech. Sym. Series, AMD 11, 1975, pp. 31–48.
4. T. A. Cruse, 'Two-dimensional BIE fracture mechanics analysis', *Appl. Math. Modeling*, **2**, 287–293 (1978).
5. T. A. Cruse and R. B. Wilson, 'Advanced applications of boundary-integral equation methods', *Nucl. Eng. Des.*, **46**, 223–234 (1978).
6. T. A. Cruse, in J. L. Swedlow (ed.), *The Surface Crack: Physical and Computational Solutions*, ASME, New York, 1972, pp. 153–170.
7. F. J. Rizzo and D. J. Shippy, 'A formulation and solution procedure for the general non-homogeneous elastic inclusion problem', *Int. J. Solids Struct.*, **4**, 1161–1173 (1968).
8. A. R. Ingraffea, G. Blandford and J. A. Liggett, 'Automatic modeling of mixed-mode fatigue and quasi-static crack propagation using the boundary element method', *Proc. 14th National Symposium of Fracture Mechanics*, ASTM STP 971, 1983, pp. 1407–1426.
9. J. C. S. Long, P. Gilmour and P. Witherspoon, 'A model for steady fluid flow in random three-dimensional networks of disc-shaped fractures', *Water Resour. Res.*, **21**, 1105–1115 (1985).
10. A. R. Ingraffea, 'Case studies of simulation of fracture in concrete dams', *Eng. Fract. Mech.*, in press.
11. L. J. Gray, 'Boundary element method for regions with thin internal cavities', *Eng. Anal.*, in press.
12. L. J. Gray, G. E. Giles and M. W. Wendel, 'Boundary element method for regions with thin internal cavities II', *Eng. Anal.*, accepted.
13. L. J. Gray and G. E. Giles, 'Application of the thin cavity method to shield calculations in electroplating', *Proc. Boundary Elements 10 Conference, Computational Mechanics*, Southampton, 1988.

14. L. J. Gray, A. L. Askew and G. E. Giles, 'Boundary element method for contact heat transfer', *Proc. of the European Boundary Element Conference*, J. L. Migeot (ed.), Université Libre de Bruxelles, Brussels, May 1988, pp. 3.21–3.36.
15. T. J. Rudolphi, G. Krishnasamy, L. W. Schmerr and F. J. Rizzo, 'On the use of strongly singular integral equations for crack problems', *Proc. Boundary Elements 10 Conference, Computational Mechanics*, Southampton, 1988, pp. 249–263.
16. N. I. Ioakimidis, 'The hypersingular integrodifferential equation of a straight crack along the interface of two bonded isotropic half-planes' *Int. J. Fract.*, **38**, R75–R79 (1988).
17. L. J. Gray, 'Evaluation of hypersingular integrals in the boundary element method', *Comp. Math. Appl.* (in press).
18. L. F. Martha, A. R. Ingraffea and L. J. Gray, 'Three-dimensional fracture simulation with a single-domain, direct boundary element formulation', in preparation.
19. F. J. Rizzo, 'An integral equation approach to boundary value problems of classical elastostatics', *Quart. Appl. Math.*, **25**, 83–95 (1967).
20. T. A. Cruse, 'Numerical solutions in three-dimensional elastostatics', *Int. J. Solids Struct.*, **5**, 1259–1274 (1969).
21. S. Mukherjee, *Boundary Element Methods in Creep and Fracture*, Applied Science Publishers, Barking, U.K., 1982.
22. H. B. Dwight, *Tables of Integrals and Other Mathematical Data*, Macmillan, New York, 1961.
23. C. F. Shih, H. G. de Lorenzi and M. D. German, 'Crack extension modelling with singular quadratic isoparametric elements', *Int. J. Fract.*, **12**, 647–651 (1976).
24. H. Tada, P. Paris and G. Irwin, *The Stress Analysis of Cracks Handbook*, Del Research Corporation, Hellertown, Pennsylvania, 1973.
25. H. Okada, H. Rajiyah and S. N. Atluri, 'A novel displacement gradient boundary element method for elastic stress analysis with high accuracy', *Trans. ASME*, **55**, 786–794 (1988).
26. W. Zang and P. Gudmundson, 'A boundary integral method for internal piece-wise smooth crack problems', *Int. J. Fract.*, **38**, 275–294 (1988).
27. M. D. G. Salomon, 'Elastic analysis of displacements and stresses induced by the mining of seam or reef deposits', *J. S. Afr. Inst. Min. Metall.*, **10**, 128–149 (1963).
28. S. L. Crouch, 'Solution of plane elasticity problems by the displacement discontinuity method', *Int. j. numer. methods eng.*, **10**, 301–342 (1976).
29. S. L. Crouch and A. M. Starfield, *Boundary Element Methods in Solid Mechanics*, George Allen & Unwin, London, 1983.
30. E. Z. Polch, T. A. Cruse and C.-J. Huang, 'Traction BIE solutions for flat cracks', *Comp. Mech.*, **2**, 253–267 (1987).